

PAPER

[View Article Online](#)
[View Journal](#) | [View Issue](#)Cite this: *RSC Sustainability*, 2023, 1, 2066

The highly selective conversion of lignin models and organosolv lignin to amines over a Ru/C catalyst†

Jin Xie,^a Xiaojing Wu,^a Jieyun Zhang,^a Xin Dai,^a Zelong Li[✉]*^a and Can Li[✉]*^{ab}

The efficient conversion of lignin into high-value chemicals is a significant and challenging process for sustainable development. In this study, we successfully achieved the direct conversion of lignin model compounds and realistic lignin into amines using H₂ and NH₃ over a Ru/C catalyst. We specifically investigated diphenyl ether (DPE) as a model molecule due to the high dissociation energy of its C–O bond, aiming to gain insights into the reaction mechanism. The results revealed that the C–O bond is initially broken, resulting in the production of benzene and phenol. Subsequently, cyclohexanone is obtained through the hydrogenation of phenol. Furthermore, cyclohexanone, acting as the key intermediate, reacts with NH₃ to yield amines. Notably, the kinetics of phenol hydrogenation to cyclohexanone is more favorable than the C–O bond cleavage of DPE. Therefore, the C–O bond rupture in lignin plays a crucial role in the depolymerization of lignin and its conversion into amines in this study. This developed strategy for lignin conversion to amines opens up new possibilities for the highly efficient utilization of lignin.

Received 20th July 2023
Accepted 7th September 2023

DOI: 10.1039/d3su00250k

rsc.li/rscsus

Sustainability spotlight

Utilizing lignin, the second most abundant organic carbon renewable resource, to produce high-value chemicals, such as amines, is a promising strategy for replacing fossil fuels. The conversion of lignin to amines could be realized through an indirect pathway, wherein lignin is first depolymerized *via* hydrogenolysis or hydrolysis, and then the resulting oxygen-containing aromatics are further converted to amines. However, the indirect pathway is limited by high energy consumption, making a direct transformation of lignin to amines necessary. This study demonstrates the feasibility of the direct transformation from lignin models and realistic lignin into amines, highlighting its significance in achieving UN SDG 12 – Responsible Consumption and Production.

Introduction

The conversion of biomass is a promising strategy for producing high value-added chemicals to replace fossil resource processes.^{1–5} Hence, the efficient utilization of lignin through the chemical pathway to provide a wide variety of chemicals is highly demanding.^{6–12} Amines are important platform molecules and have been widely applied in the manufacture of dyes, drugs, *etc.*^{13,14} The synthesis routes for amines start from fossil fuels as carbon sources, which are obtained through steam or catalytic cracking, leading to the emission of massive amounts of CO₂ (Fig. 1).¹⁵ Therefore, well-designed reaction pathways can realize highly efficient conversion of lignin to

chemicals, which can afford critical chemical commodities and decrease the emission of CO₂.

70% of structural units in lignin are linked through aromatic carbon–oxygen (C–O) bonds and the dominant types of C–O bonds in lignin include α -O-4, β -O-4, and 4-O-5 linkages

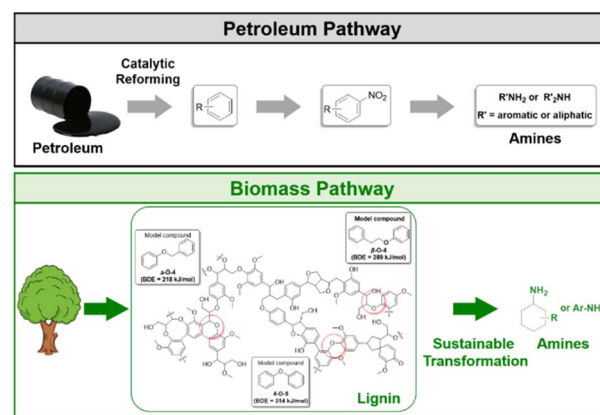


Fig. 1 The processes of the transformation from petroleum and lignin to amines.

^aKey Laboratory of Advanced Catalysis, State Key Laboratory of Applied Organic Chemistry, College of Chemistry and Chemical Engineering, Lanzhou University, Lanzhou, Gansu 730000, China. E-mail: Lizl@lzu.edu.cn; canli@lzu.edu.cn

^bState Key Laboratory of Catalysis, Dalian Institute of Chemical Physics, Chinese Academy of Sciences, Dalian National Laboratory for Clean Energy, Dalian, Liaoning 116023, China

† Electronic supplementary information (ESI) available. See DOI: <https://doi.org/10.1039/d3su00250k>

(Fig. 1).^{16,17} The conversion of lignin to amines can be realized through the indirect pathway, in which the C–O bonds were ruptured firstly through hydrogenolysis or hydrolysis and then the obtained oxygen-containing aromatics were converted to amines.^{15,18–26} However, the indirect pathway requires high energy consumption to realize the conversion of lignin to amines because of the separation process for every step. Therefore, it is necessary to develop a direct pathway to convert lignin to amines. It is known that the rupture of the C–O bonds in lignin and the conversion of oxygen-containing intermediates are crucial for the direct conversion of lignin to amines according to the indirect pathway. Hence, the model compounds of three main C–O bond linkages in lignin, including 4-O-5 (bond dissociation energy (BDE) = 314 kJ mol^{−1}), α -O-4 (BDE = 218 kJ mol^{−1}) and β -O-4 (BDE = 289 kJ mol^{−1}) linkages,²⁷ were used as substrates to investigate the conversion pathway of lignin to amines (Fig. S1†). Pd catalysts exhibit good catalytic activity for the direct transformation of DPE (4-O-5 linkage model) and benzyl phenyl ether (BPE, α -O-4 linkage model) to amines *via* the combination of reductive cleavage of the C–O bond and the subsequent amination.^{28–31} However, the Pd catalysts require the use of a Lewis acid (LA) as the co-catalyst. Compared to the β -O-4 alcohol models, the β -O-4 ketone models, obtained through chemoselective oxidation or dehydrogenation of β -O-4 alcohol models, exhibit a higher activity in their reaction with nitrogen-containing compounds, resulting in the production of amines or amides.^{32–39} The oxidation and dehydrogenation strategy can facilitate the conversion of β -O-4 linkage models into amines; however, these methods are unable to promote the conversion of α -O-4 and 4-O-5 linkage models. Therefore, developing a highly efficient strategy to directly convert these three linkage models to amines is necessary for realizing the conversion of realistic lignin into value-added amines.

Herein, the direct conversion of lignin C–O bond model compounds, including α -O-4, β -O-4, and 4-O-5 linkages, to amines was realized with H₂ and NH₃ over a Ru/C catalyst. The results of DPE (with the highest BDE compared to the other two linkages) conversion show that the hydrogenolysis of the C–O bond occurs first, and then the obtained phenol can be hydrogenated to cyclohexanone and cyclohexanol; the cyclohexanone as the important intermediate reacts with NH₃ for the synthesis of amines. It is found that the hydrogenolysis of the C–O bond of DPE is more difficult than the hydrogenation of phenol to cyclohexanone over Ru/C in kinetics. Furthermore, the organosolv birch lignin could also be transformed into amine compounds efficiently with the Ru/C–H₂–NH₃ catalytic system.

Results and discussion

Initially, DPE was employed as the substrate to investigate the conversion of lignin dimers to primary amines (Table 1). Pd/C catalyst fails to promote the DPE conversion (Table 1, entry 1), and Pt/C and Rh/C provide inferior conversion (Table 1, entries 2 and 3). To our delight, Ru/C could convert DPE to cyclohexylamine (CYAM) with high activity and selectivity (99% conversion, 43% selectivity to CYAM, and 22% selectivity to benzene

(Ben), Table 1, entry 4). Reducing the loading of Ru/C leads to a slight decrease in DPE conversion but provides higher selectivity to CYAM and Ben (92% conversion, 45% selectivity to CYAM, and 37% selectivity to Ben, Table 1, entry 5). With the absence of H₂, the DPE could not be converted, indicating that H₂ is necessary during the conversion of DPE (Table 1, entry 6). Finally, Ru/C was chosen as the optimal catalyst for further investigations. The Ru/C catalyst was subsequently characterized, and the results can be found in the ESI (Fig. S2†).

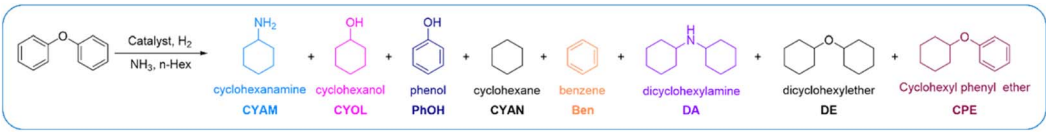
The reaction conditions, including the reaction temperature (Fig. S3†) and H₂ pressure (Fig. S4†), were optimized to further improve the reactivity. The results suggest that the conversion is dependent on the reaction temperature. With increasing the reaction temperature from 140 °C to 200 °C, the DPE conversion increases from 13% to 92%, and the selectivity has no significant change (Fig. S3†). The H₂ pressure affects the reaction conversion and selectivity significantly. The DPE conversion increases from 4% to 97% when the total pressure increases from 1.0 MPa (0.8 MPa NH₃ and 0.2 MPa H₂) to 5.0 MPa (0.8 MPa NH₃ and 4.2 MPa H₂), and the selectivity to CYAM and Ben decreases obviously with increased pressure, and with 3 MPa total pressure (0.8 MPa NH₃ and 2.2 MPa H₂), the selectivity to Ben and CYAM increases to 82% (Fig. S4†). Based on the results above, the optimized reaction conditions were determined to be 25 mg 5 wt% Ru/C, 2.5 mmol lignin models, 3 MPa total pressure (0.8 MPa NH₃ and 2.2 MPa H₂), and 200 °C for 2 hours.

Under the optimal reaction conditions, the reaction mechanism was further investigated. The product distributions of the DPE transformation as a function of time at 200 °C in the H₂–NH₃ atmosphere (H₂ pressure: 2.2 MPa, NH₃ pressure: 0.8 MPa) are shown in Fig. 2a. At the beginning of the reaction (reaction time t = 15 min), Ben and CYAM are the main products; the selectivity to Ben is 45% and decreases to 36% with the reaction time being prolonged, indicating Ben further transformed to cyclohexane (CYAN) with 12% selectivity. The selectivity to CYAM is 21% at the reaction time t = 15 min and increases to 43% after reaction time t = 60 min, and the selectivity to cyclohexanol (CYOL) decreases from 14% to 4% with the reaction time being prolonged (Fig. 2a). These results above indicated that the conversion of DPE to CYAM was initiated through the hydrogenolysis of DPE. The yields of Ben and CYAM increased with the reaction time being prolonged (Fig. 2b), indicating that the oxygenated monomers obtained from the DPE hydrogenolysis will further react with ammonia to afford CYAM.

The yield of CYOL increases first and then starts to decrease with the highest value at the reaction time of 30 min, meaning the CYOL was further transformed to CYAM (Fig. 2c). The phenol (PhOH) reaches 1.25% yield at reaction time t = 30 min, then decreases to 0.8% with prolonged reaction time, indicating PhOH also has been further converted (Fig. 2c). In addition, the cyclohexyl phenyl ether (CPE) synthesized through the hydrogenation of DPE is also detected with 5% selectivity. It is possible that the Ben and CYOL may be derived through the hydrogenolysis of the CPE intermediate but not directly derived from the DPE hydrogenolysis. However, it hardly reacts for the



Table 1 Conversion of DPE under different conditions^a

										
Entry	Catalyst	Conv. ^b (%)	Sel. ^b (%)							
			CYAM	CYOL	PhOH	CYAN	Ben	DA	DE	CPE
1	5 wt% Pd/C	N.R.	—	—	—	—	—	—	—	—
2	5 wt% Pt/C	2.5	0	18.2	0	29.8	4.1	0	12.8	35.1
3	5 wt% Rh/C	10.9	27.5	1.1	10.1	5.1	34.6	0.6	2.3	18.7
4	5 wt% Ru/C	99	43.0	5.4	0	25.1	22.2	0.6	0.5	3.2
5 ^c	5 wt% Ru/C	92	44.6	4.8	0	10.5	37.0	0.4	0.1	2.6
6 ^d	5 wt% Ru/C	NR	—	—	—	—	—	—	—	—

^a Reaction conditions: 50 mg catalyst, *n*-hexane (5 mL), DPE (425 mg, 2.5 mmol), NH₃ (0.8 MPa), H₂ (2.2 MPa), temperature (200 °C), reaction time: 3 hours. ^b The conversion and selectivity were determined by GC. ^c 25 mg 5 wt% Ru/C. ^d Ar (30 bar at RT) was used to replace H₂. The entries labeled with “—” indicate that the concentrations were below the detection limits of the method.

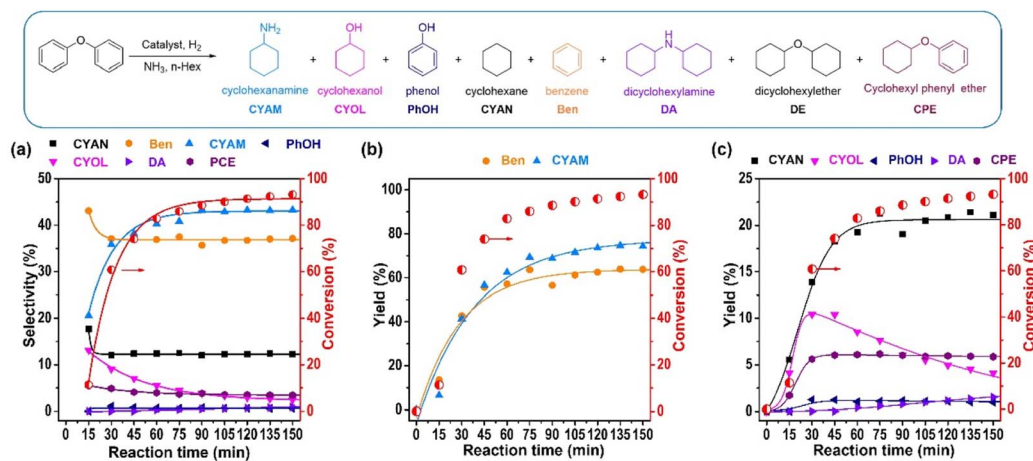


Fig. 2 DPE transformation product distributions and DPE conversion as a function of reaction time over Ru/C. (a) For DPE conversion and product selectivity; (b) for DPE conversion and product distributions of Ben and CYAM; (c) for DPE conversion and product distributions of CYAN, cyclohexanol (CYOL), PhOH, dicyclohexylamine (DA), and CPE. Reaction conditions: DPE (4-O-5) (5.1 g, 0.030 mol), 5 wt% Ru/C (0.300 g, 7.42 × 10⁻⁵ mol of Ru), *n*-hexane (60 mL), 200 °C, 0.8 MPa NH₃, 2.2 MPa H₂, stirring at 600 rpm.

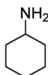
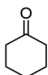
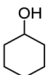
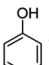
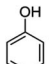
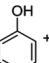
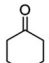
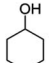
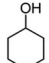
conversion of CPE under H₂ and NH₃ over Ru/C catalyst (Scheme S1†). It is well known that CYAN and CYOL can be produced through the hydrogenation of Ben and phenol (PhOH) respectively.^{40,41} These results suggest that the hydrogenolysis of DPE is the main reaction under H₂ and NH₃ over Ru/C, which is more difficult than the transformation of oxygenated intermediates to amines, and the CYOL shows a crucial role in the production of CYAM.

According to the results of kinetics, it is evident that CYOL plays a role as an intermediate in the formation of CYAM. It is known that PhOH and Ben are the products of DPE hydrogenolysis. CYOL and cyclohexanone (CYON) can be generated through the hydrogenation of PhOH. Consequently, it is possible that CYAM is formed through the reaction of NH₃ with PhOH, CYOL, or CYON, respectively. Therefore, control experiments

were conducted to identify the key intermediates during the conversion of DPE to CYAM by calculating the apparent turnover frequencies (ATOFs) and the apparent energy barrier (*E*_a) (Fig. S5†). The PhOH can be hydrogenated to CYON and CYOL under H₂, which displays high activity with an ATOF of 3.13 s⁻¹, and the *E*_a is 48.2 kJ mol⁻¹ (Table 2, entry 1), indicating that the PhOH can be easily hydrogenated to CYON and CYOL under the reaction conditions. When NH₃ was introduced into the reaction system of PhOH hydrogenation, the main product changed from CYON to CYAM, the reaction rate decreased with an ATOF of 0.65 s⁻¹, and the *E*_a is 184.1 kJ mol⁻¹ (Table 2, entry 2). In the absence of H₂, the reaction between PhOH and NH₃ is hardly converted (Table 2, entry 3), suggesting that the CYON and CYOL are the possible intermediates for the conversion of PhOH with NH₃ to amines. The main product for the reaction of CYOL with NH₃ is



Table 2 Control experiments of oxygenated intermediates^{a,i}

Entry	Substrates	Conv. ^b (%)	Sel. ^b (%)			ATOF ^c (s ⁻¹)	E _a (kJ mol ⁻¹)
							
1 ^{d,e}	 + H ₂	23	—	74	26	3.13	48.2
2	 + H ₂ + NH ₃	12	85	—	15	0.65	184.1
3	 + NH ₃	NR	—	—	—	—	—
4 ^{d,f}	 + H ₂ + NH ₃	10	97	—	3	2.27	89.2
5	 + H ₂ + NH ₃	6	99	—	—	0.32	200.5
6 ^g	 + H ₂ + NH ₃	NR	—	—	—	—	—

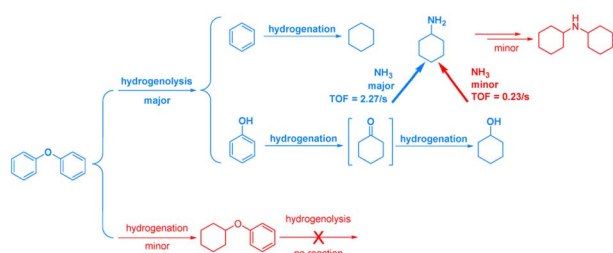
^a Reaction conditions: 10 mg 5 wt% Ru/C catalyst, *n*-hexane (10 mL), oxygenated intermediate (20 mmol), NH₃ (0.8 MPa), H₂ (2.2 MPa), temperature (200 °C), reaction time: 25 min. ^b The conversion and selectivity were determined by GC. ^c The apparent turnover frequency values (ATOFs) were calculated on the basis of the Ru content when the conversion is not more than 25%. ^d 5 mg 5 wt% Ru/C was loaded. ^e Reaction time: 20 min. ^f Reaction time: 10 min. ^g Without catalyst. ⁱ The entries labeled with “—” indicate that the concentrations were below the detection limits of the method, and “NR” indicates no reaction.

the CYAM with a selectivity of 99%; this reaction shows an ATOF of 0.32 s⁻¹, and the E_a is 200.5 kJ mol⁻¹ (Table 2, entry 5). In contrast, the main product for the reaction of CYON with NH₃ is also CYAM with a selectivity of 97% (Table 2, entry 4), the ATOF is 2.27 s⁻¹, which is 7 times that of the reaction for CYOL with NH₃, and the E_a is 89.2 kJ mol⁻¹, which is less than one half that of the reaction for CYOL with NH₃. These results indicate that the PhOH is first hydrogenated to CYON, and then CYON as the main component reacts with NH₃ to synthesize the amines. Based on the results above, the reaction pathway for conversion of DPE with NH₃ to amines is proposed as follows (Scheme 1): (1) the Ben and PhOH are generated from DPE hydrogenolysis; (2) the PhOH can be hydrogenated to CYON and CYOL; (3) compared with CYOL, CYON as the main component reacts with

NH₃ for the production of CYAM; (4) the partial Ben can be hydrogenated to CYAN.

The conversion of other lignin model molecules to amines was also investigated, and the reaction results are shown in Table 3. These reactions show high activity as well. For DPE (4-O-5), CYAM is generated in 85% yield, and Ben is obtained in 69% yield (Table 3, entry 1). The conversion of BPE (α-O-4 linkage model molecule) affords a 75% yield of CYAM and an 85% yield of toluene (Table 3, entry 2). For PPE (β-O-4 linkage model molecule), 55% CYAM and 69% ethylbenzene are obtained (Table 3, entry 3). The conversion of 2-phenoxy-1-phenylethan-1-ol (β-O-4 linkage model molecule, Table 3, entry 4) provides CYAM with 56% yield. The conversion of 2-phenoxy-1-phenylethan-1-one (β-O-4 linkage model molecule, Table 3, entry 5) shows a more complex distribution of products. Besides the yield of CYAM being 33%, the other amines are also obtained through the reductive amination of carbonyl compounds. These results indicate that the Ru/C–H₂–NH₃ system is active for the cleavage and amination of lignin's 4-O-5, α-O-4, and β-O-4 linkages. Finally, the stability of Ru/C was tested for the conversion of DPE to amines (Fig. S6†). The Ru/C catalyst shows good stability without obvious deactivation after being used 5 times.

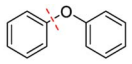


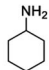
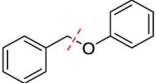
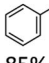
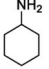
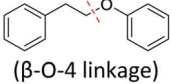
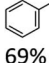
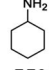
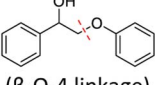
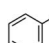
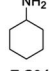
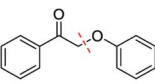
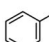
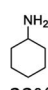
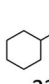
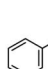
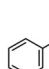
After the test of lignin models, the production of amines from the conversion of realistic lignin was investigated (Fig. 3). Firstly, the birch sawdust was treated through methanolysis,



Scheme 1 The proposed reaction pathway of DPE (the model for 4-O-5 bond linkage in lignin) transformation with Ru/C as the catalyst.



Table 3 Reaction of lignin model compounds with ammonia catalyzed by Ru/C^a

Entry	Substrate	Reaction time (h)	Conv. ^b (%)	Main products and yields ^b
1	 (4-O-5 linkage)	2	92	 23%  69%  85%
2	 (α-O-4 linkage)	11	95	 85%  75%
3	 (β-O-4 linkage)	6	86	 69%  55%
4	 (β-O-4 linkage)	6	91	 41%  56%
5	 (β-O-4 linkage)	6	99	 24%  33%  23%  17%  22%

^a Reaction conditions: 25 mg catalyst, *n*-hexane (5 mL), substrate (2.5 mmol), 0.8 MPa NH₃, 2.2 MPa H₂, 200 °C. ^b The conversion and yield were determined by GC.



Fig. 3 The conversion of realistic organosolv lignin to amines.

leading to a 9.0% yield of the organosolv lignin (detailed information can be found in the ESI†). Subsequently, direct conversion of organosolv birch lignin with Ru/C–H₂–NH₃ was conducted. The 2D ¹³C–¹H HSQC NMR results were employed to investigate the depolymerization of organosolv lignin. Compared with the HSQC spectra of organosolv lignin before reaction (Fig. S7b, S8a, and S9a†), the significant depolymerization of organosolv lignin (Fig. S8b†) and the cleavage of dominant C–O–C bonds in lignin (Fig. S9b†) are observed, indicating the conversion of organosolv lignin with the Ru/C–H₂–NH₃ catalytic system. For confirming the formation of the amines, the hydrogenolysis of organosolv lignin was investigated under H₂ over the Ru/C catalyst (Ru/C–H₂ catalytic system), and the hydrogenolysis result displays the depolymerization of organosolv lignin (Fig. S7c, S8c, and S9c†) while the obtained products are very different under these two reaction systems with or without NH₃, suggesting the formation of amines with NH₃ for depolymerization of organosolv lignin.

Compared with the HSQC spectrum result for cyclohexylamine (Fig. S7d†), the cyclohexylamine derivatives are found to have been produced with the Ru/C–H₂–NH₃ system (Fig. S7a†). The results of gas chromatography-mass spectrometry (GC-MS) analysis indicate that the detected monomers after depolymerization for the Ru/C–H₂ system are mainly alcohol and phenolic monomers (Fig. S10–S16†), and a 7.6% yield of aliphatic primary amines is obtained after the depolymerization of organosolv lignin with the Ru/C–H₂–NH₃ system (Fig. S10 and S17–S22†).

Conclusions

In summary, an efficient strategy of heterogeneous catalytic one-pot conversion of lignin ether model compounds to primary amines was developed successfully. The investigation of DPE as a model molecule shows that the C–O bond of DPE is ruptured firstly and then the produced PhOH is hydrogenated



to CYON and CYOL; CYON plays a key role in the production of amines under H_2 and NH_3 over Ru/C. The lignin model compounds including α -O-4, β -O-4, and 4-O-5 linkages can be converted with this highly efficient catalytic system. This suggests that the depolymerization of organosolv lignin undergoes the rupture of C–O bonds as the important step for depolymerization of lignin and then the obtained oxygen-containing intermediates can be hydrogenated and then react with NH_3 for the synthesis of the amines. In addition, the direct conversion of the organosolv lignin to amines was realized with H_2 and NH_3 over the Ru/C catalyst, and a 7.6% yield of amines was obtained. This work develops the reaction system and reveals the reaction mechanism for the formation of amines, which are conducive to designing the highly efficient catalytic system for the depolymerization of organosolv lignin.

Conflicts of interest

There are no conflicts to declare.

Acknowledgements

This work was conducted by the National Key Research and Development Program of China (2021YFA1501101) and the Fundamental Research Funds for the Central Universities (lzujbky-2019-pd02 and lzujbky-2019-60).

References

- 1 P. Gallezot, *Chem. Soc. Rev.*, 2012, **41**, 1538–1558.
- 2 C. O. Tuck, E. Pérez, I. T. Horváth, R. A. Sheldon and M. Poliakoff, *Science*, 2012, **337**, 695–699.
- 3 M. I. Besson, P. Gallezot and C. Pinel, *Chem. Rev.*, 2014, **114**, 1827–1870.
- 4 R. A. Sheldon, *Green Chem.*, 2014, **16**, 950–963.
- 5 R. A. Sheldon and J. M. Woodley, *Chem. Rev.*, 2018, **118**, 801–838.
- 6 M. Zaheer and R. Kempe, *ACS Catal.*, 2015, **5**, 1675–1684.
- 7 M. V. Galkin and J. S. Samec, *ChemSusChem*, 2016, **9**, 1544–1558.
- 8 S. Gillet, M. Aguedo, L. Petitjean, A. Morais, A. da Costa Lopes, R. Łukasik and P. Anastas, *Green Chem.*, 2017, **19**, 4200–4233.
- 9 W. Schutyser, a. T. Renders, S. Van den Bosch, S.-F. Koelewijn, G. Beckham and B. F. Sels, *Chem. Soc. Rev.*, 2018, **47**, 852–908.
- 10 Z. Sun, B. Fridrich, A. De Santi, S. Elangovan and K. Barta, *Chem. Rev.*, 2018, **118**, 614–678.
- 11 C. Chio, M. Sain and W. Qin, *Renewable Sustainable Energy Rev.*, 2019, **107**, 232–249.
- 12 S. S. Wong, R. Shu, J. Zhang, H. Liu and N. Yan, *Chem. Soc. Rev.*, 2020, **49**, 5510–5560.
- 13 K. Hunger, P. Mischke, W. Rieper, R. Raue, K. Kunde and A. Engel, in *Ullmann's Encyclopedia of Industrial Chemistry*, 2000.
- 14 S. D. Roughley and A. M. Jordan, *J. Med. Chem.*, 2011, **54**, 3451–3479.
- 15 M. Pelckmans, T. Renders, S. Van de Vyver and B. F. Sels, *Green Chem.*, 2017, **19**, 5303–5331.
- 16 Z. Chen and C. Wan, *Renewable Sustainable Energy Rev.*, 2017, **73**, 610–621.
- 17 A. Shivhare, D. Jampaiah, S. K. Bhargava, A. F. Lee, R. Srivastava and K. Wilson, *ACS Sustainable Chem. Eng.*, 2021, **9**, 3379–3407.
- 18 Z. Chen, H. Zeng, S. A. Girard, F. Wang, N. Chen and C.-J. Li, *Angew. Chem., Int. Ed.*, 2015, **54**, 14487–14491.
- 19 Z. Chen, H. Zeng, H. Gong, H. Wang and C.-J. Li, *Chem. Sci.*, 2015, **6**, 4174–4178.
- 20 Z. Sun, G. Bottari, A. Afanasenko, M. C. A. Stuart, P. J. Deuss, B. Fridrich and K. Barta, *Nat. Catal.*, 2018, **1**, 82–92.
- 21 P. Tomkins, C. Valgaeren, K. Adriaensen, T. Cuyppers and D. E. D. Vos, *ChemCatChem*, 2018, **10**, 3689–3693.
- 22 E. Blondiaux, J. Bomon, M. Smoleń, N. Kaval, F. Lemièrre, S. Sergeev, L. Diels, B. Sels and B. U. W. Maes, *ACS Sustainable Chem. Eng.*, 2019, **7**, 6906–6916.
- 23 Y. Liu, A. Afanasenko, S. Elangovan, Z. Sun and K. Barta, *ACS Sustainable Chem. Eng.*, 2019, **7**, 11267–11274.
- 24 Z. Qiu, L. Lv, J. Li, C.-C. Li and C.-J. Li, *Chem. Sci.*, 2019, **10**, 4775–4781.
- 25 T. Cuyppers, T. Morias, S. Windels, C. Marquez, C. Van Goethem, I. Vankelecom and D. E. De Vos, *Green Chem.*, 2020, **22**, 1884–1893.
- 26 X. Liu, W. Chen, J. Zou, L. Ye and Y. Yuan, *ACS Sustainable Chem. Eng.*, 2022, **10**, 6988–6998.
- 27 J. He, C. Zhao and J. A. Lercher, *J. Am. Chem. Soc.*, 2012, **134**, 20768–20775.
- 28 X. Cui, K. Junge and M. Beller, *ACS Catal.*, 2016, **6**, 7834–7838.
- 29 B. Zheng, J. Song, H. Wu, S. Han, J. Zhai, K. Zhang, W. Wu, C. Xu, M. He and B. Han, *Green Chem.*, 2021, **23**, 268–273.
- 30 H. Zeng, D. Cao, Z. Qiu and C.-J. Li, *Angew. Chem., Int. Ed.*, 2018, **57**, 3752–3757.
- 31 D. Cao, H. Zeng and C.-J. Li, *ACS Catal.*, 2018, **8**, 8873–8878.
- 32 Y. Liu, Q. Luo, Q. Qiang, H. Wang, Y. Ding, C. Wang, J. Xiao, C. Li and T. Zhang, *ChemSusChem*, 2022, **15**, e202201401.
- 33 H. Li, M. Liu, H. Liu, N. Luo, C. Zhang and F. Wang, *ChemSusChem*, 2020, **13**, 4660–4665.
- 34 X. Liu, H. Zhang, C. Wu, Z. Liu, Y. Chen, B. Yu and Z. Liu, *New J. Chem.*, 2018, **42**, 1223–1227.
- 35 J. Zhang, Y. Liu, S. Chiba and T.-P. Loh, *Chem. Commun.*, 2013, **49**, 11439–11441.
- 36 B. Zhang, T. Guo, Y. Liu, F. E. Kühn, C. Wang, Z. K. Zhao, J. Xiao, C. Li and T. Zhang, *Angew. Chem., Int. Ed.*, 2021, **60**, 20666–20671.
- 37 Y. Ding, T. Guo, Z. Li, B. Zhang, F. E. Kühn, C. Liu, J. Zhang, D. Xu, M. Lei, T. Zhang and C. Li, *Angew. Chem., Int. Ed.*, 2022, **61**, e202206284.
- 38 H. Li, M. Wang, H. Liu, N. Luo, J. Lu, C. Zhang and F. Wang, *ACS Sustainable Chem. Eng.*, 2018, **6**, 3748–3753.
- 39 H. Li, A. Bunrit, J. Lu, Z. Gao, N. Luo, H. Liu and F. Wang, *ACS Catal.*, 2019, **9**, 8843–8851.
- 40 H. Liu, T. Jiang, B. Han, S. Liang and Y. Zhou, *Science*, 2009, **326**, 1250–1252.
- 41 Y. Wang, J. Yao, H. Li, D. Su and M. Antonietti, *J. Am. Chem. Soc.*, 2011, **133**, 2362–2365.

